We are IntechOpen,
the world's leading publisher of
Open Access books
Built by scientists, for scientists

6,900
Open access books available

186,000
International authors and editors

200M
Downloads

154
Countries delivered to

Our authors are among the

TOP 1%
most cited scientists

12.2%
Contributors from top 500 universities

CLARIVATE ANALYTICS
BOOK CITATION INDEX
INDEXED

WEB OF SCIENCE™

Selection of our books indexed in the Book Citation Index
in Web of Science™ Core Collection (BKCI)

Interested in publishing with us?
Contact book.department@intechopen.com

Improving Iris Recognition Performance Using Quality Measures

Nadia Feddaoui, Hela Mahersia and Kamel Hamrouni

LSTS Laboratory, National Engineering School of Tunis, University ElManar
Tunisia

1. Introduction

Biometric methods, which identify people based on physical or behavioural characteristics, are of interest because people cannot forget or lose their physical characteristics in the way that they can lose passwords or identity cards. Among these biometric methods, iris is currently considered as one of the most reliable biometrics because of its unique texture's random variation. Moreover, iris is proved to be well protected from the external environment behind the cornea, relatively easy to acquire and stable all over the person's life. For all of these reasons, iris patterns become interesting as an alternative approach to reliable visual recognition of persons. This recognition system involves four main modules: iris acquisition, iris segmentation and normalization, feature extraction and encoding and finally matching.

However, we noticed that almost all the iris recognition systems proceed without controlling the iris image's quality. Naturally, poor image's quality degrades significantly the performance of the recognition system. Thus, an extra module, measuring the quality of the input iris, must be added to ensure that only "good iris" will be treated by the system. The proposed module will be able to detect and discard the faulty images obtained in the segmentation process or which not have enough information to identify person. In literature, most of evaluation quality methods have developed indices to quantify occlusion, focus, contrast, illumination and angular deformation. These measurements are sensitive to segmentation errors. Only few methods have interested on the evaluation of iris segmentation.

This chapter aims to present, firstly a novel iris recognition method based on multi-channel Gabor filtering and Uniform Local Binary Patterns (ULBP), then to define a quality evaluation method which integrates additional module to the typical recognition system.

Proposed method is tested on Casia v3 iris database. Our experiments illustrate the effectiveness and robustness of ULBP to extract rich local and global information of iris texture when combined with simultaneously multi-blocks and multi-channel method. Also, obtained results show an improvement of iris recognition system by incorporating proposed quality measures in the typical system.

This chapter is organized as follows: Section 2 describe in details the proposed iris recognition system. The further represents the quality evaluation method. In section 4, we expose experiments, results and comparison. Finally, the conclusion is given in section 5.

2. Iris recognition system

In a typical iris recognition system, the eye image is preprocessed to obtain a segmented and normalized image, then its texture is analysed and encoded to form an iris features vector 'template'. Finally, we compare templates to estimate similarity between irises.

2.1 Iris preprocessing

Iris preprocessing step includes iris segmentation and iris normalization.

Iris segmentation aims to isolate iris texture from the acquired eye image, with exclusion of any obscuring elements such as eyelids, eyelashes (Fig. 1-a), and reflections from the cornea or possibly from eyeglasses. Various methods have been proposed to accomplish this task (Daugman, 1994, Wildes, 1997, Daugman, 2007, Liu, 2006, Krichen, 2007).

In the proposed method, we modelled the iris and pupil by two circles not necessarily concentric and eyelids by two segments of line. Different borders are located by the application of Hough transform. Then, we have applied the pseudo polar transformation of Daugman to transform the iris arc from raw coordinates (x,y) to a doubly dimensionless and non concentric coordinate system (r, θ) (Fig. 1-b). The details were described in (Feddaoui & Hamrouni, 2010).

Since, the result is not well contrasted, it is better to enhance the textured image before analyzing its texture (Fig. 1-c). According to result obtained in the segmentation step, we note that the area belonging to [π/6..11π/6] is generally disturbed by the presence of eyelids and eyelashes and consequently, the most discriminating information of texture is in the other portion of the iris. Moreover, in order to reduce the impact of reflection in this region, we don't consider texture present in the 1/6 internal portion (Fig. 1-d).
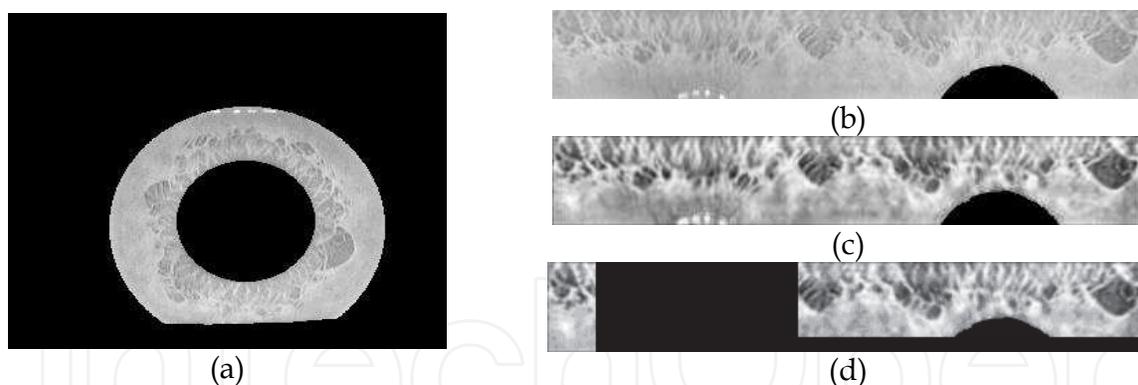

Fig. 1. Iris normalization (a) Segmented iris image (b) Rectangular iris image (c) Enhanced iris image (d) Region of interest in iris image

2.2 Iris texture analysis

In an iris recognition system, the feature extraction and encoding aims to represent the details of the iris texture by finding efficient and discriminative descriptors that are resistant to large variation in illumination, rotation, occlusions, deformation and other factors which disturb the iris texture. There are various methods proposed since the pioneer work of Daugman, in 1992 (Duagman, 1994). Gabor filters (Duagman, 2006) (Masek, 2003) (Ma et al., 2002) (Huang et al., 2007) (Feddaoui & Hamrouni, 2009, 2010) and wavelet (Lim et al., 2001) (Krichen et al., 2004) has shown very good performance because of their capability to multi-

scale representation. Gabor features encode edge information and texture shape of iris texture over a range of multiple narrow-band frequency and orientation components.

In this chapter, we proposed a novel method to extract iris features combining Gabor filters and ULBP operators. The LBP operator succeeds in many applications where it is combined with multi-resolution methods. It has proved its high discriminative power for texture analysis where employed with Cosine Transform (Ellaroussi et al., 2009) and Gabor wavelet in (Zhang et al., 2009) (Tan & Triggs, 2007) to face recognition, Wavelet Packet Transform (Qureshi, 2008) in medical image analysis, Haar wavelet transform (Wang et al., 2008) to ear recognition and Steerable Pyramid (Montoya et al., 2008) to texture analysis.

2.2.1 Proposed method

In the proposed method, we analyzed iris texture by Uniform Local Gabor Patterns ULGP which can be defined as an application of ULBP operators to the Gabor representation. The main components of the proposed method can be summarized as follows:

- Represent global spatial texture information by application of a set of Gabor filters on iris image

In spatial domain, the Gabor function in the spatial domain is a Gaussian modulated sinusoid. For a 2-D Gaussian curve with a spread of σ_x and σ_y in the x and y directions, the 2-D Gabor function is given by equation 1 and the real impulse response of the filter is presented in equation 2 (Bovic et al., 1990).

$$h(x,y) = \frac{1}{2\pi\sigma_x\sigma_y}\exp\left\{-\frac{1}{2}\left[\frac{x'^2}{\sigma_x^2}+\frac{y'^2}{\sigma_y^2}\right]\right\}\exp\left(2\pi ifx'\right) \tag{1}$$

$$h_r(x,y) = \frac{1}{2\pi\sigma_x\sigma_y}\exp\left\{-\frac{1}{2}\left[\frac{x'^2}{\sigma_x^2}+\frac{y'^2}{\sigma_y^2}\right]\right\}\cos(2\pi fx') \tag{2}$$

Where

$$\begin{pmatrix} x' \\ y' \end{pmatrix} = \begin{pmatrix} \cos\theta & \sin\theta \\ -\sin\theta & \cos\theta \end{pmatrix}\begin{pmatrix} x \\ y \end{pmatrix}$$

In the frequency domain, the equations (3) and (4) represent respectively the frequency response of the complex and real Gabor filters.

$$G(u,v) = \exp\left\{-2\pi^2\left[(u-f)^2\sigma_x^2+v^2\sigma_y^2\right]\right\} \tag{3}$$

$$G_r(u,v) = \exp\left\{-2\pi^2\left[(u-f)^2\sigma_x^2+v^2\sigma_y^2\right]\right\} + \exp\left\{-2\pi^2\left[(u+f)^2\sigma_x^2+v^2\sigma_y^2\right]\right\} \tag{4}$$

In our application, we have applied a bank of Gabor filters on iris image. We have chosen 4 frequencies (2, 4, 8, 16) and 4 orientations (0°, 45°, 90°, 135°) which generated a total of 16

filtered images. The space constant σ is chosen to be inversely proportional to the central frequency of the channels.

- Compute ULBP operators in each filtered image to encode local variation across different Gabor coefficients in defined radius.

Actually, LBP operator is one of the best texture feature descriptor and it has already proven its high discriminative power for texture analysis. The original version of the LBP operator was introduced by Ojiala *et al.*, it capture the micro-features in the image by encoding them in a 3x3 local window and thresholding eight neighbours pixels with the value of the central pixel, then a binomial factor of 2^i is assigned for each pixel. The LBP code is computed by summing the results of multiplying the thresholded value by a corresponding weight (Ojala et al., 1996). The process is summarized in Fig. 2.
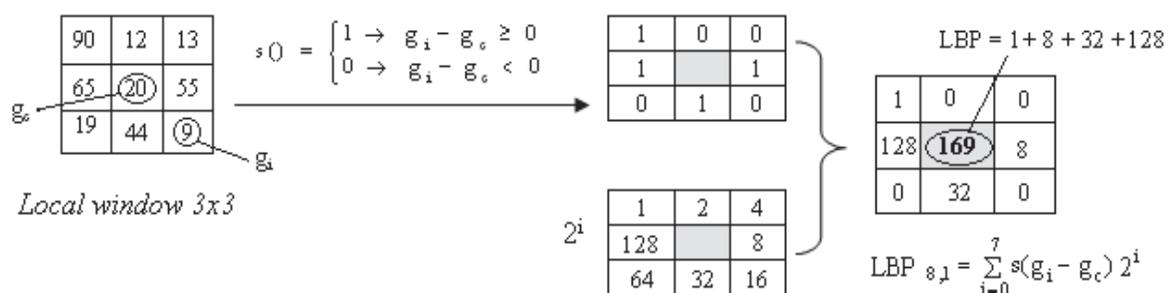

Fig. 2. The original version of LBP

Later, The conventional LBP operator has been extended to introduce a robust illumination and orientation invariant texture feature by computing the pixel values that lie on a circular pattern with a radius *r* around the central pixel. ULBP represent the most common LBP codes without significant loss in its discrimination capability. It reduces the 256 different local binary patterns defined in a 3 x 3 neighbourhoods to 10 by representing the number of bitwise spatial transitions (0/1) in a circular pattern. To quantify these ULBP (equation 5), an uniformity measure *U* was introduced (equation 6)

$$ULBP = \begin{cases} \sum_{i=0}^{7} s(g_i - g_c) & if \quad U(LBP) \le 2 \\ 9 & otherwise \end{cases} \tag{5}$$

$$U(LBP) = \left| S(g_{i-1} - g_c) - S(g_0 - g_c) \right| + \sum_{i=0}^{7} \left| S(g_i - g_c) - S(g_{i-1} - g_c) \right| \tag{6}$$

- Extract the global and local signatures by first dividing each obtained image into non-overlapping blocks having a given size, then computing statistical features within each block to form a vector.

This step aims to extract appropriate texture features from ULGP representations. The idea is to divide the whole ULGP image into blocks having a given size. Then, to provide a good discriminating feature between irises. In this paper, we have proposed to compute statistical features on each ULGP representation. Finally, features are concatenated to form the complete feature vector which size varies depending on the block size (5x5, 10x10, 20x20, 30x30).

- Form iris template by encoding local relationship between measures of vector.

This step aims to generate iris template based on representing the features variations. First, we have linearized the matrix of statistical features then each coefficient is compared to the previous one and is encoded by 1 or 0: 1 if it is greater than the previous one and 0 otherwise. This process is similar to the computation of the derivative of the feature vector and the encoding of its sign. In practice, this binary iris code facilitates greatly the matching process.

Since persons are identified by their templates, the process of person verification needs a comparison between two templates in order to estimate their similarity. Considering that the iris is represented by a binary template, the Hamming distance is more suitable to estimate the difference between iris patterns with a bit-by-bit comparison.

The computation of the Hamming distance is given by the following expression:

$$HD = \frac{\|(A \otimes B) \cap MaskA \cap MaskB\|}{\|MaskA \cap MaskB\|} \tag{7}$$

Where {A,B} are the two templates and {MaskA, MaskB} their corresponding noise masks.

In our algorithm, we obtained rotation invariance by unwrapping the iris ring at different initial angles. Five initial angle values are used in experiments [-4°, -2°,0, 2°, 4°]. Thus, we defined five images for each iris class in the data base. And when matching the input feature code with a class, the minimum of the scores is taken as the final matching distance.

3. Quality evaluation method

Actually, the function of the iris recognition system is affected by the quality of used images. When the images used are not of a high quality, this affects significantly the performances, one has to discover the images of poor quality and to separate them.

An image of poor quality complicates the segmentation phase proved by the difficulty of detecting the different borders of iris, consequently the presence of the non detected noise in the iris texture. This noise affects the results of different stages of a recognition system particularly the stage of texture analysis, that can be also affected by the focus of the image and even the nature of the texture. In fact, the iris texture must include enough information to identify person.

To select images of good quality, we have developed a model quality that evaluates the results of segmentation and the richness of texture. The model is integrated in the recognition system after the phase of segmentation. Based on generated qualities measures, we process in the characterization stage, only image that surpass a certain threshold. The choice of its value depends of the security level of the intended application.

In the following section, we introduce the principal woks made to evaluate the quality of iris image.

3.1 State of art

During the last decade, many works have been interested in the evaluation of the quality of an iris image. Despite the diversity of the applied methods, they proved experimentally an improvement of the recognition system performance.

Most of these works defined the quality in terms of texture clarity, focus degree, occlusion rate, dilation degree, view angle, etc. The used techniques can be classified into 3 categories:

those operating in the Fourier Domain, those based on 2D wavelets transform and the statistical methods.

3.1.1 Quality measures in the frequential domain

The choice of indices quality measurement in the frequential domain is justified by the fact that an out-of-focus image can be considered as a result of the filtering of the ideal image by a low pass filter, and then the main part of information of texture is located in the low frequencies. On the contrary, this information is between the low and high frequencies for clear image.

Daugman estimated the clarity of iris image in term of the rate of the energy of high components. This energy increases proportionally to the degree of focus image (Daugman, 2004). Ma et al. analyzed the frequential distribution of the two areas of size 64x64 pixels around the pupil. Then, the quality indices are used by a SVM classifier for the training and the classification of images in 4 categories: clear images, out-of-focus images, blurred images due to the eye movement during the acquisition and images altered by the presence of eyelids and eyelashes (Ma et al., 2003).

Later, Kalka et al. studied many other factors on the system performance such as: the occlusion, the pupil dilation, the illumination, the percentage of significant pixels, the movement of eye, the reflections, the view angle and the distance from the camera. According to their study, the focus, the eye movement and the view angle degrade more the performances. They analyzed the high frequency components to measure the degree of blur due to camera distance and the directional properties of the Fourier spectrum for the blur due to the movement (Kalka et al., 2006). To evaluate the angle of view, they measured the circularity of iris by applying an integro-differential operator to different images obtained by projecting the original image at different angles. So, the angle of correction maximizes this operator.

Tissé has implemented 12 techniques proposed in the literature, to evaluate the clarity of iris image, based on: gradient , wavelets, filter, etc. He compared the obtained indices on an analysis region, he deduced that the method based on FSWM filters (Frequency Selective Weighted Median Filter) leads the better results (Tissé, 2007). In the same year, Ketchantang et al. proposed an index of image quality in a sequence of images acquired in real time. This measure combines the speed of the pupil moving between two successive frames, the density of dark pixels in the pupil area and the clarity of the collarette. The speed of displacement is estimated by using Kalman filter. This operator provides informations about the quantity of blur caused by the sudden movement of the eye during the acquisition.

The density of dark pixels in the pupil estimates the depth of focus. The clarity of the collarette is evaluated in the Fourier domain by measuring the energy of middle frequency components of a region around the pupil (Ketchantang et al., 2007).

3.1.2 Quality measures based on wavelet transform

Generally, the algorithms operating in the frequency domain are applied on the entire image (or an interest region), hence they are sensitive to the noise and give a global sight of the focus degree of the iris texture. To solve these problems, many solutions applied the 2D wavelets transform to produce a local descriptor of the iris quality. Chen et al. suggested a local measure of quality based on the « Mexican Hat » wavelet transform. The segmented iris image is divided into multiple concentric bands with a fixed width, around the pupil.

The degree of blur of each band is measured by the energy of the wavelet coefficients. Then, a global index of quality was defined as a weighted average of the local quality measurements. The weight reflects the distance of the candidate band relative to the pupil (Chen et al., 2006).

In order to enhance iris image, Vatsa et al. used a discret wavelet transform DWT and a SVM classifier on a set of 8 images that incorporates the original iris image and its transformed one by 7 known enhancement algorithms such as the histogram equalization, the entropy equalization, etc. the DWT is applied on each image, and the coefficients of the approximation and details bands are classified as coefficients of good quality by SVM classifier (Vatsa et al., 2008).

3.1.3 Quality measures based on statistical measures

In addition to the techniques described above, several researchers have considered statistical measures to assess the quality of iris images. Zhang et al. filed a patent concerning the process that determines whether the image is focused correctly. It is based on analyzing the shape and the continuity of the iris boundary. They considered a number of lines crossing the pupil boundary, for each line, statistical values are calculated for the pixels belonging either to the pupil and the iris (Zhang et al., 1999).

Proença et al. developed a method based on statistical measures and neural networks. The process consists in calculating 5 statistical measures in 7x7 windows derived from a segmented polar iris image. The measures commonly used are: ASM (Angular Second Moments), entropy, contrast, energy and inertia. Then, a simple thresholding of index computed in each analysis window permit the classification of central pixel into "noisy" or "significant" pixel (Proença & Alexandre, 2006).

Cambier et al. studied the impact of 7 quality measures on the performance of a recognition system for multi-cameras recognition system. These index are the iris and pupil radius, the pupil-iris ratio, the iris-sclera contrast, the iris intensity, the texture energy and the percentage of visible iris. Results showed that the texture energy and the rate of visible iris are the most important but specific to population (Cambier & Seelen, 2006).

Krichen introduced a statistical model GMM (Gaussian Markov Model) to define a global quality score estimating that iris image represents a good quality texture (Krichen., 2007).

To determine whether the image has enough information to identify person, Belcher et al. (Belcher & Du, 2008) and Zhou et al. (Zhou et al.,2009) developed a quality index by combining 3 index: the dilation score, the occlusion score and the feature information score. Iris image is segmented then the texture is analyzed by Log-Gabor filters. A global feature information score is estimated by averaging the entropy information distance between pairs of consecutive rows of the filtered image. This quality measure was used by Y. Du et al (Du et al, 2010) to evaluate the quality of a compressed iris image. In fact, during compression, iris patterns are replaced by new artificial patterns, and only the most distinctive iris patterns resist. These false patterns are too correlated compared to the original image and they become more important through compression rate. Consequently, the more compression rate is elevated, iris texture quality becomes weaker.

Based on the fact that the inner region of iris contain more discriminative patterns, Sung et al. improved the matching performance by merely weighting the inner and outer iris regions with respectively 1 and 0 (Sung et al., 2007).

In the cited works, the quality measures are often computed in the segmented images which makes them sensitive to the segmentation errors. In practice, no segmentation method has a

rate of 100% of correct segmentation. Nevertheless, the study of Zhou et al. is among the rare that took into account the evaluation of the segmentation results of an iris image (Zhou et al., 2009). This is because the segmentation of the iris has specific particularities and existing methods for evaluating the segmentation (Chabier et al., 2005) (Foliguet & Guigues, 2006) are not applicable in this case. In (Zhou et al.,2009), Zhou et al evaluated the segmentation accuracy in terms of localizing correctly the center and boundary of pupil and the iris boundary including the limbic boundary and the eyelid boundaries. This measure is based on the analysis of the histogram of a rectangular horizontal area including the two centres, three sub-regions belonging to pupil, iris and sclera.

3.2 Proposed method for quality evaluation

A typical biometric system includes 4 stages: the capture of the eye, the segmentation and normalization of iris image, the texture analysis and encoding and finally the matching.

A too noisy image or poorly segmented is processed in all system steps which often leads to a false identity recognition. Thus, the proposed system consists of integrating a quality module after the segmentation step. The objective of this module is to select images to be processed in the system. For this, we developed two quality units: the first one assess the result of segmentation while the second estimates the richness of texture.

Fig. 3 illustrates different units of the given system and the following sections describe every module.
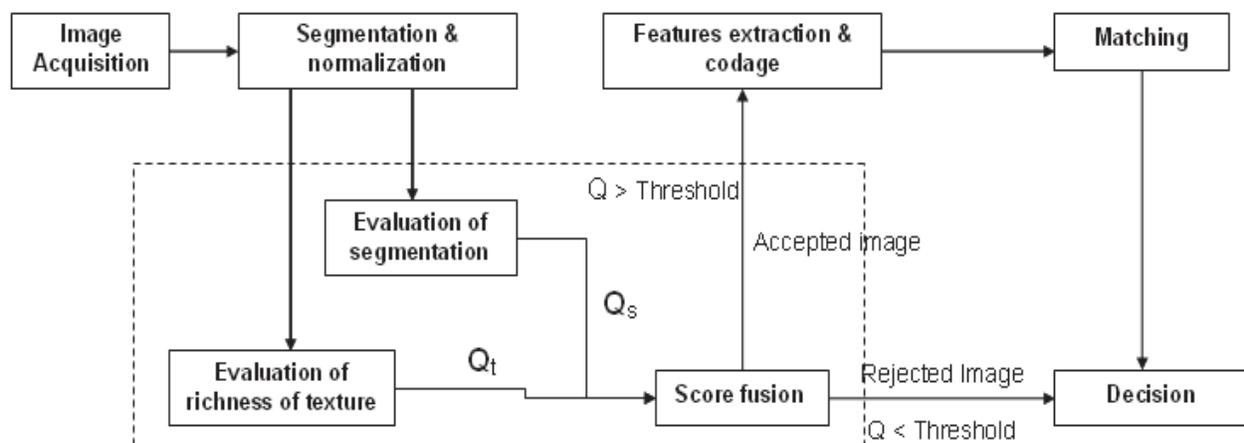

Fig. 3. Proposed iris recognition system: integration of quality units in typical system

3.3 Evaluation of the segmentation

This unit aims to verify if the image is correctly segmented. It takes as input the coordinates of the pupil and iris and the generated masks, then it analyzes each detected boundary in order to estimate the corresponding quality index.

3.3.1 Evaluation of the pupil boundary

The first stage in the segmentation process is the localisation of the pupil, which results influences the performance of the rest of system. In practice, an inadequate segmentation of the pupil alters the content of the iris arc by adding or eliminating a portion of the pupil located near the border. Fig. 4-a illustrates the relationship between the matching distance and the pupil radius. We can see that the correct segmented image (R) produces a low

similarity distance whereas the bad localized pupil (R-8, R-4, R+4,R+8) degrades significantly the distance.
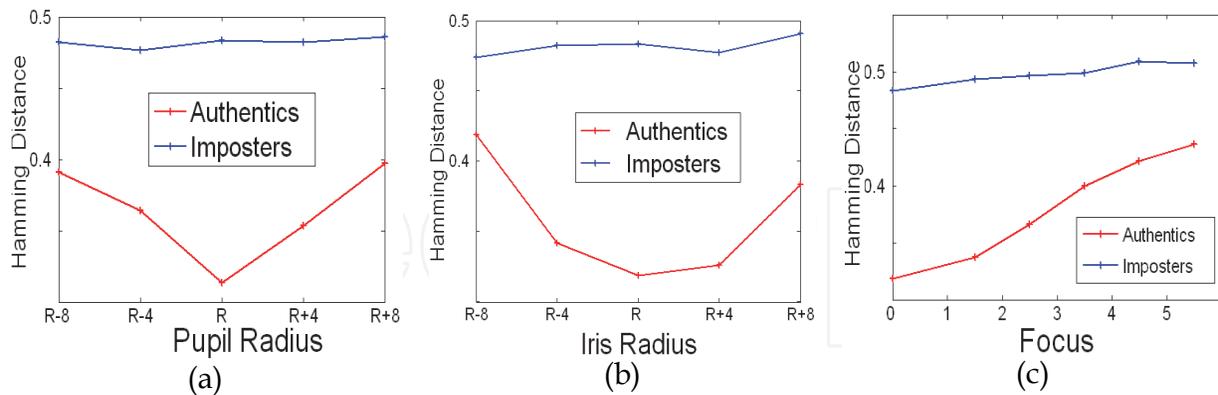

Fig. 4. Illustration of the relationship between the distance between two feature vectors and (a) the pupil radius (b) the iris radius (c) the richness of iris texture

These errors are mainly caused by the physiological nature of the iris and the lighting conditions during acquisition. In fact, the pupil is not perfectly circular or elliptical and always presents fluctuations and discontinuities along its border (Fig. 5). Also, the pupil is often partially hidden under the light spots and the eyelashes. the proximity of the noise to the pupil border increasingly complicates the segmentation process.

(a)   (b)

Fig. 5. Illustration of the fluctuation of the pupil boundary relative to the detected border (white line): (a) segmented pupil image (b) border region in polar coordinates.

To estimate this defect, we generate an index evaluating the quality of segmentation through the following steps:
- Minimize the effect of light spots by filling the clear holes by the average of the image intensity
- Consider a region located on both sides of the detected border.
- Filter this region, then analyze the pupil fluctuations across the detected circle boundaries in order to determine the real mask of the pupil ($Mask_{real}$). In fact, we added to the detected mask ($Mask_{detect}$) during segmentation the non-detected pixels located outside the detected pupil, and we eliminate the invalid pixels belonging to the iris arc and located inside the detected pupil.
- Apply equation (8) to measure a quality index Q_p assessing the pupil segmentation:

$$Q_p = 1 - \frac{\|Mask_{real} \otimes Mask_{\det ect}\|}{\|Mask_{\det ect}\|} \tag{8}$$

3.3.2 Evaluation of iris/sclera boundary

The segmentation evaluation depends not only on the pupil localization but also on the iris boundary, which should separate the iris from eyelids and sclera. In this unit, we are interested in the iris/sclera boundary.

To show the impact of an adequate boundary detection on iris texture, we represent in Fig. 6, three polar images (b-c-d) that are relative to image (a) by considering 3 different iris radius. We can notice that the segmentation errors generally caused a significant destruction of texture patterns and consequently a wrong distance between iris codes. The relationship between the iris radius and this distance is illustrates in Fig. 6-b. We can see a clear degradation of distance with inadequate iris radius (R-4, R-8, R+4, R+8).
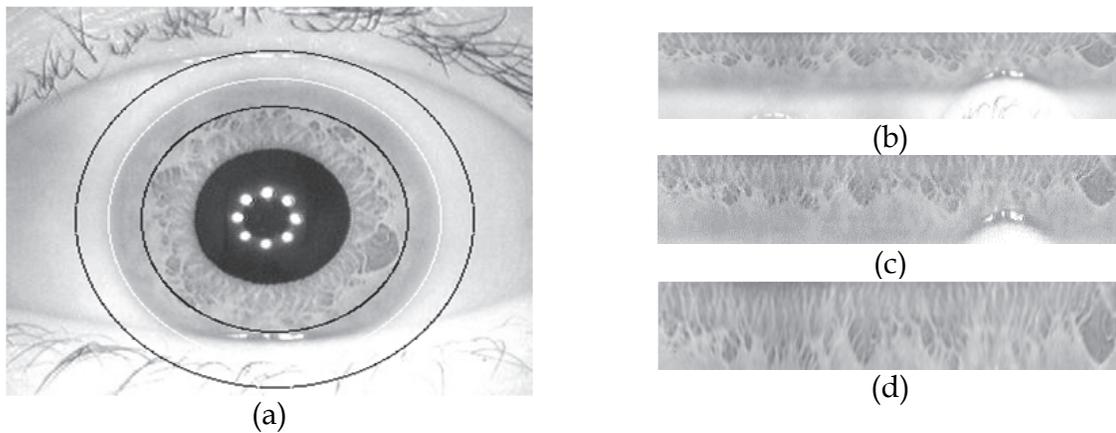

Fig. 6. The impact of the iris/sclera boundary on iris texture: original image (a) , polar image by considering adequate radius (c) and inadequate radius (c-d): the segmentation errors caused a significant destruction of texture patterns

In practice, the intensity variation between the region of iris and the sclera is important in perfect conditions of acquisition, which facilitates the border detection process. However, the reasons that might complicate this detection are diverse, we mainly cited the eyelashes occlusion, the lighting conditions, the percentage of visible iris and the view angle. In fact, the three first factors generates false contours that alter region boundaries. Despite the percentage of visible iris and the view angle should be reasonable to consider an important iris region in the segmentation process.

The evaluation of the iris boundary is performed in two eye regions respectively within the following ranges: [-30 ° .. 30 °] and [150 ° .. 210 °] relative to the iris center. The pixels are divided on both sides of the detected boundary (l_{detect}). Then, each region is subdivided into overlapping rectangular blocks of size hxw. A vertical projection is determined for each bloc. Then, we calculate the pixels average of every column. The obtained curve represents a minimum at the correct boundary of the iris (l_{thresh}). Its position can be localized by the maximum of the derivative of the curve. The distance separating the two positions l_{thresh} and l_{detect} is used to define a local index which assess the quality of iris boundary.

We notice that in the case of a correct segmentation, l_{thresh} and l_{detect} are confused. the process steps are described in the following algorithm:

- m=0: Number of blocks apt for the evaluation
- Subdivide the region of analysis R into n overlapping rectangular blocks B_i of size hxl. R={ B_i, i=1..n}.
For each block B_i **do**
 - Count the number of noisy pixels N_{ps}
 if $N_{ps} > \dfrac{h * l}{2}$ **then**
  - Consider the B_i inapt for the evaluation
 else
  for each row $j \in [1..h]$ of the block B_i **do**
   - Compute the average of the significant pixels m_j
  end
  - m=m+1
  - Calculate the projection $hist_i$ of obtained averages{mj} (Fig. 7.a-c)
  - Calculate the derivative of projection (Fig. 7. b-d).
  - Detect the first peak l_{thresh} in the derivative
  - Measure a local index of quality Q_i

$$Q_i = 1 - \frac{|l_{thresh} - l_{det\,ect}|}{rayon_{iris}} \qquad (9)$$

 end
end
- Evaluate the global index of quality Q_{isc} based on the local index {Q_{ij}}

$$Q_{isc} = \frac{1}{m} \sum_{i=1}^{m} Q_i \qquad (10)$$

Algorithm 1. Evaluation of iris/sclera boundary process

3.3.3 Evaluation eyelids boundaries

After the iris image segmentation, it is important to localize the eyelids occlusion. The quality of the result depends on the presence of eyelashes, glare and light spots on the eyelids borders and also the richness of texture.

In practice, these factors caused defects in contrast and false contours in the segmentation region, which don't lead to a perfect segmentation for all iris cases. To evaluate the error, we have developed a module to analyze the eyelid borders in the polar iris image. We concentrated on the low eyelid since we considered, in the next steps of the recognition process, a region of interest RI between [π/6..5π/6] (Fig. 8-b).

Algorithm 2. represents the proposed method, it is consist of analyzing the intensity variation in local windows of the regions of interest (RI) which are selected near and on the border of the detected eyelid boundary (Fig. 8-c). We computed statistical measures like standard deviation, variance, average absolute deviation, mean, entropy, etc. Tests showed that the variance gave the best results.
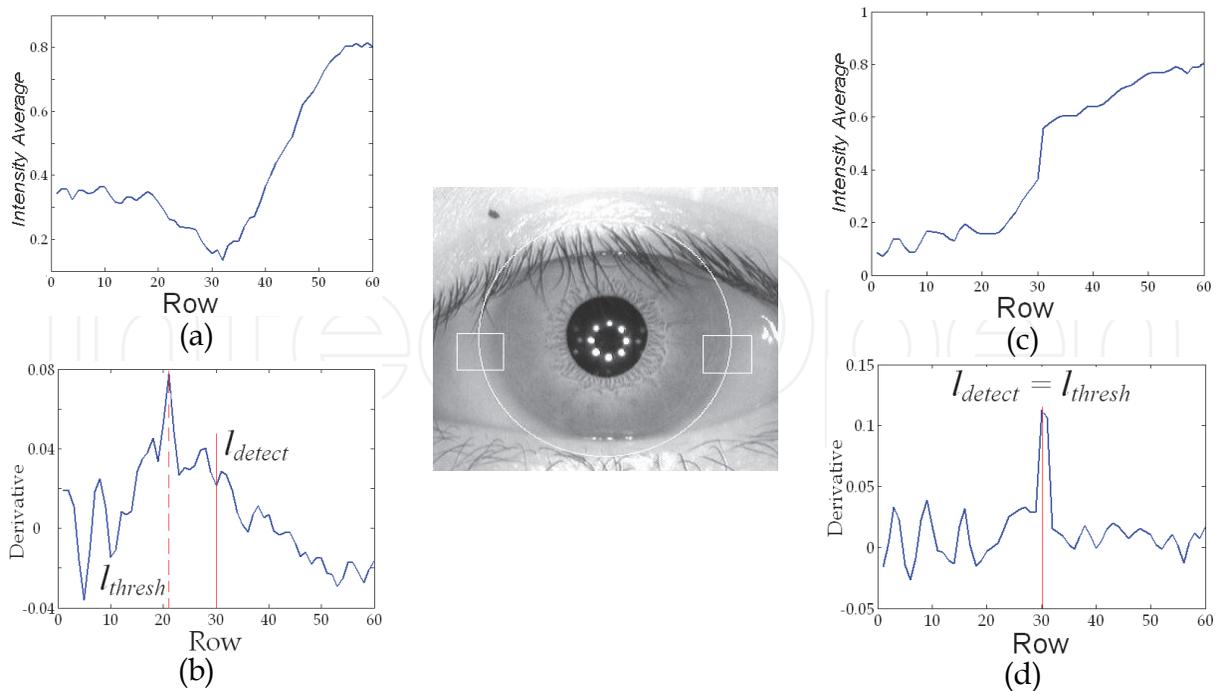
Fig. 7. Illustration of the iris boundary evaluation process: we analyze the vertical projection and its derivative of the local windows: (a-b) correspond to left region and (c-d) related to the right region. We notice that in the case of a correct segmentation, l$_{thresh}$ and l$_{detect}$ are confused.

---

if iris is not occluded by eyelids **then**

    - Assign 100% to the eyelid quality score : $Q_e = 100\%$

else

    - Subdivide the region of analysis of n overlapping blocks B_i^c (i=1..n) of size hxl. It is distributed on both sides ode detected boundary (Fig. 8-c).

    For each block B_i^c **do**

    - Consider a neighbour region B_i^v of the same size

    - Compute V_i^c and V_i^v the variances respectively of B_i^c and B_i^v :

$$V(B_i) = \frac{1}{h*l} \sum_{j=1}^{h} \sum_{k=1}^{l} \left(B_i(j,k) - \overline{B_i}\right)^2 \tag{11}$$

$$\overline{B_i} = \frac{1}{h*l} \sum_{j=1}^{h} \sum_{k=1}^{l} B_i(j,k) \tag{12}$$

    end

    - Calculate the eyelid quality score:

$$Q_e = \frac{\sum_{i=1}^{n} V_i^c}{\sum_{i=1}^{n} V_i^c + \sum_{i=1}^{n} V_i^v} \tag{13}$$

End

Algorithm 2. Evaluation of eyelid boundary process

Based on local measures, we generated a global quality index Q_e evaluating the segmentation of the lower eyelid. The index penalizes under-segmentation of the eyelid. In fact, considering the noisy pixels in the region of analysis affects the system performance more than the elimination of pixels due to the over-segmentation.
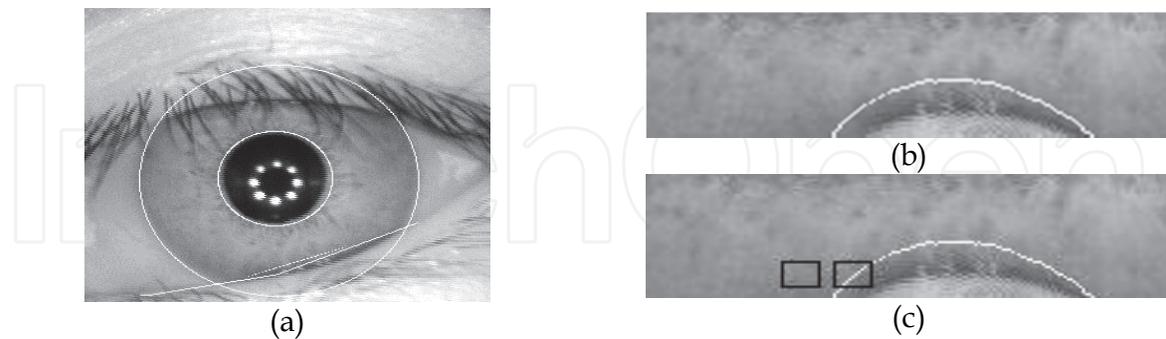
Fig. 8. Illustration of eyelids boundary evaluation (a) segmented iris image (b) segmented RI in polar coordinates (c) selection of two neighbours blocks near and on the detected boundary

3.3.4 Fusion of the segmentation scores

The global assessment of the segmentation depends on the 3 index Q_e, Q_p and Q_{isc} relating respectively to the boundary of eyelid, pupil and iris/sclera. Fig. 9 illustrates the correlation of different obtained scores. We notice that the measures are not grouped on the diagonal, which asserts that they are not correlated.
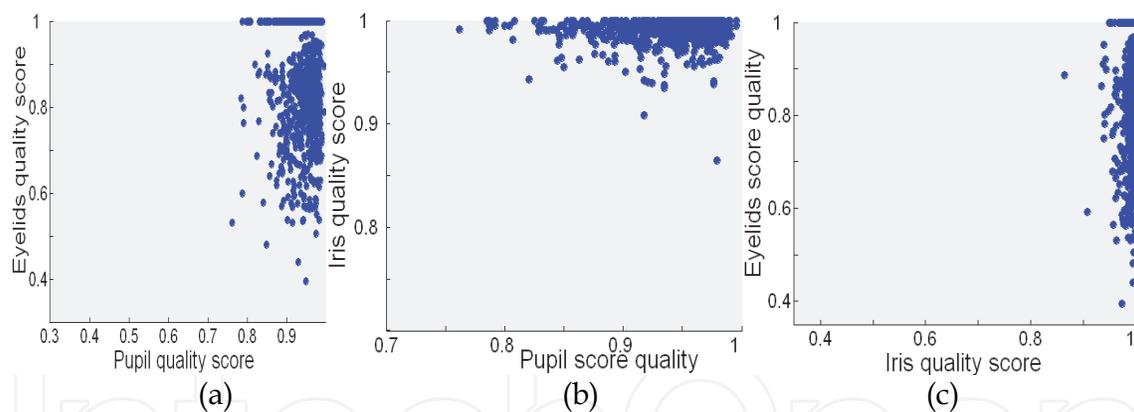
Fig. 9. Illustration of the correlations between different quality scores: the measures are not grouped on the diagonal, therefore they are uncorrelated

Since, they are all important to judge the segmentation, we average their values to generate a global index Q_s:

$$Q_s = (f_1(Q_p) + f_2(Q_{isc}) + f_3(Q_e)) / 3 \qquad (14)$$

Inspired by the work (Zhou et al., 2009), f1, f2 and f3 are parameterized functions of normalization related to the function f defined as follows:

$$f(Q) \begin{cases} 1 & Q \ge \beta \\ e^{-\alpha(\beta-Q)} & 0 \le Q < \beta \end{cases} \qquad (15)$$

The choice of an exponential function is justified in (Zhou et al., 2009) (Du et al., 2010) (Belcher & Du, 2008) by proving that the relationship between the recognition rate and the degradation factors is not linear.

In this equation, parameter ß illustrates the minimum error above which the system performance is not degraded. In fact, tests have shown that we can neglect the weak error of segmentation because it doesn't affect significantly the recognition rate. We set ß to 0.9, 097 and 0.9 for respectively f1, f2 and f3. While the parameter α represents the weight of the error on the recognition results. We have assigned more weight to Qp because poor detection of the pupil affects mainly the area that contains the most discriminative iris texture.

Given that biometry by iris is often used in high security system, we chose α = 50 for f1 in order to quickly extend the normalized score to 0 when Q_p is less than 80%. Also, we fixed α to 20 and 13 for f2 and f3 to obtain zero as normalized score when Q_{isc} and Q_e are respectively less than 70% and 50%.

3.4 Evaluation of the richness of texture

This module aims to generate a score expressing the richness of iris texture to verify if the RI of iris image has enough information to identify a person. This module is integrated into the recognition process after the image segmentation and normalization unit. It estimates a global quality index based on the following index: the occlusion score Q_o , the dilation score Q_d and the degree of texture information Q_f.

3.4.1 Occlusion score

The amount of available iris region can affect the recognition performance. In this unit, we developed an occlusion score Q_o estimating the percentage of significant pixels of the RI. This index is evaluated as follows:

$$Q_o = \frac{N_{ps}}{N} \tag{16}$$

Where N is the total number of pixels of RI and N_{ps} is the number of significant pixels of RI.

3.4.2 Dilation score

In a recognition system, the pupil dilation may affect performance. This is explained by the fact that the shape and the density of texture patterns are altered by the degree of iris deformation. In this paper, we developed an evaluation dilation unit which takes as input the pupil radius R_p and the iris radius R_i to compute the dilation score Q_d as follows:

$$Q_d = 1 - \frac{R_p}{R_i} \tag{17}$$

3.4.3 Estimation of texture information

When the iris image is slightly noisy and correctly segmented, the recognition problems related to the texture information. Whatever the adopted algorithm, its robustness depends on the richness of texture that varies from a subject to another. Fig. 10 gives examples of this

diversity. The texture details are presented in the frequency domain by high frequency components.
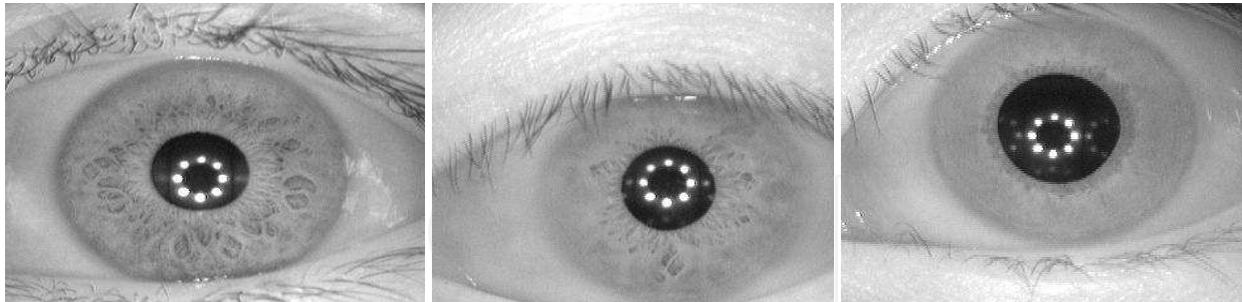

Fig. 10. Examples of the diversity of iris texture

Generally, the blur is appears as a loss of information as a smooth texture patterns, a bad separation between different iris patterns and a distortion of fine edges.

For that, we studied the evolution of the similarity distance between iris according to the different degradation of the texture information. We simulated this degradation by a low pass Gaussian filter with an increased mask size. Fig. 4-c shows a clear degradation of distances especially between genuine iris. In fact, an important amount of texture details are destroyed when the size of the filter mask is larger. This makes necessary to classify the iris in function of the amount of texture information and separate the clear images of blurred images. In addition, from a technical point of view, it is not possible to derive a clear iris image from a blurred one. Correcting the contrast can improve its quality.

All these problems require taking into account the texture information measure in the recognition process, to ensure a good selection of images.

In section (3.1), we presented some proposed texture information measures in literature. In order to ensure a good estimation of the texture richness and an acceptable computation time, we proposed a global quality index operating in the cosine transform (DCT) field.

This transform was used by Matej et al. to estimate the focus of a sequence of images taken in different conditions. They demonstrated the efficiency of the DCT compared to other existing methods and its robustness against the noise occlusion. In fact, a good evaluation of the focus has been achieved even when an artificial noise was added. (Matej et al., 2006)

This work helps us to develop a global index of texture information based on the shanon's entropy and the energy's distribution of DCT coefficients.

3.4.3.1 Cosine transform of an image

Cosine transform, (CT or DCT for digital cosine transform), is a linear mathematical transformation similar to the discrete Fourier transform, it was introduced in 1974 by Ahmed et al. to reduce redundancy information. A DCT expresses a sequence of cosine functions which generates real coefficients, and therefore it avoids the complex numbers as in the case of the Fourier transform. (Ahmed et al., 1974)

The DCT is often used in signal and image processing and especially in audio and video compression. The standards MPEG, JPEG and MJPEG apply the DCT in the compression process. However, DCT is commonly used in image processing to obtain the spectral representation of the digital image.

Given an image I of size MxN, the DCT transform provides an image R of the same dimension. This transformation represents an interest because it concentrates the major part

of energy in a minimum of low coefficients. Thus, an adequate use of this information leads to a good analysis of the candidate image. We can locate these low-frequency coefficients in the top left corner of the image (Fig. 14.d-e-f). Whereas the other coefficients in the corner right bottom of the image may be neglected and reduced to zero in the compression process. It is known that the Discrete Fourier Transform DFT is used by several algorithms for estimating the focus of an image. However, in the last decade, the DCT has been increasingly used by the visual systems that the DFT, and this is thanks to its high concentration of energy in some low-frequency coefficients. In addition, the basic function of DFT is exponential and generates complex coefficients therefore it requires a computation time greater than the DCT.

Moreover, Krotkov and Yeo et al. suggest in (Krottov, 1987) (Yeo et al., 1993) that the DFT contains information that is superfluous to the focus evaluation such as the phase information. For these reasons we preferred the DCT to measure the blur in image.

In practice, this optimal transformation is sensitive to contrast changes, so this defect may be limited by the image preprocessing or the normalization of the transformed image by DCT.

|		
(a)	(b)	(c)
(d)	(e)	(f)
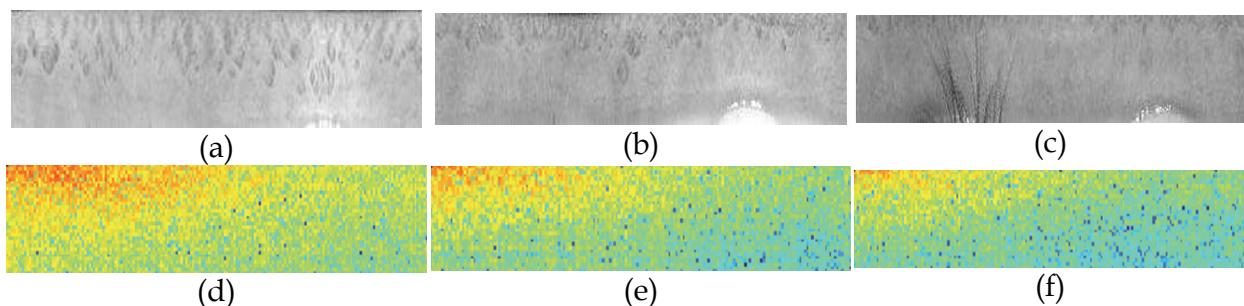
Fig. 11. Illustration of the relationship between the richness of iris texture and the normalized DCT: for visualization purposes, we display in (d-e-f) the logarithm of the transformed images. The coefficients with higher values are shown in red. By comparing the images (d-e-f), we notice that the spectrum of sharp image is more uniform. Quality measures obtained are respectively: 0.76, 0.33 and 0.21.

3.4.3.2 Implementation

To evaluate the texture information, we developed a global quality index, based on the DCT representation of the iris image and the entropy of the energy distribution. For optimization purposes, the proposed method is based on an existing solution adopted by the compression standard JPEG, by applying the DCT in 8x8 blocks. Indeed, it was proven that the choice of this block size is a good compromise between quality and computation time (Pennebaker & Mitchell., 1992). Algorithm 3 summarizes the proposed procedure to evaluate a global texture information index Q_f. Fig. 11. illustrates the application of normalized DCT to three polar iris images (a-b-c). For the visualization purposes, we considered the logarithm of the transform in (d-e-f) images. When comparing these images, we can deduce that the image with highest texture information produces more uniform spectrum than others. In fact, the less sharp image concentrates more energy in a minimum coefficient of low coordinates. We obtained respectively the quality measures: 76%, 33% and 21%, which shows that the uniformity measure of the spectral representation of image is appropriate for estimating the texture information.

- Consider a region of analysis R of size 48x240
- Subdivide R into n non-overlapping blocks B_i of size 8x8. R={ B_i, i=1..n}.
for each block B_i **do**
      - Compute R the DCT of B_i. R(B_i)={Rpq, p=1..8,q=1..8}
      - Calculate R' the normalize DCT of B_i. R'(B_i)={R'$_{pq}$} is defined as follows:

$$R'_{pq}(B_i) = \frac{R_{pq}(B_i)}{\sum\limits_{p} \sum\limits_{q} R_{pq}(B_i)} \tag{18}$$

      - Estimate a local texture information score $Q_f(B_i)$ by computing the energy of B_i

$$Q_f(B_i) = \frac{1}{64} \sum_{p} \sum_{q} (R'_{pq}(B_i))^2 \tag{19}$$

 end
 - Evaluate a global texture information score $Q_f(I)$ by computing the entropy of Shannon of local measures {$Q_f(B_i), i = 1..n$}. The entropy describe the energies distribution of the energies of the standardized TCD image.

$$Q_f(I) = -\sum_{i=1}^{nb} Q_f(B_i) \log(Q_f(B_i)) \tag{20}$$

Algorithm 3. Evaluation of texture information process

3.4.4 Scores fusion

To estimate the richness of texture, we generated a global quality index Q_t by averaging the three generated quality scores Q_o, Q_d and Q_f, respectively related to the occlusion, the dilation and the texture information. We started by normalizing these scores in [0 .. 1] by the function (6).

According to several experiments, we concluded that the image quality is not affected when the occlusion rate doesn't surpass 10%, the dilation score is less than 40% and the sharpness score overcomes the 50%. Despite that, the image is inadequate when the dilation score becomes 75% or the occlusion rate overcomes 60% or the sharpness score is less than 35%. So, the normalized scores tend to 0 when the corresponding threshold are reached.

3.5 Estimation of global quality score

In this part, we generated a global quality score Q which takes into consideration the amount of available region and the efficiency of information contained in the iris image. These criteria have already been evaluated by the quality scores Q_s and Q_t. The validation of these measures on the basis Casia v3 shows that both are important for quality assessment also they are uncorrelated, then they were combined by averaging their value.

4. Experimentations and results

4.1 Iris database

In order to evaluated the accuracy of the proposed method, extensive experiments on Casia v3 iris images are performed.

Currently, Casia v3 presents the largest iris database available in public domain. It has been released to more than 2 900 users from 70 countries since 2006. CASIAv3 includes three subsets which are labelled as CASIA-IrisV3-Interval, CASIA-IrisV3-Lamp, CASIA-IrisV3-Twins. All iris images are 8 bit gray-level JPEG files with 280x320 of resolution and collected under near infrared illumination in different times. Most of the images were captured in two sessions, with at least one month interval and the specula reflections from the NIR illuminators on the iris texture introduce more intra-class variations (Casia, 2006).

To validate our method, we have considered 2641 images of 249 people in CASIA-IrisV3-Interval database.

4.2 System evaluation

The experiments are completed in verification mode (one-to-one). In this system, the two compared templates are similar and represent the same iris if the distance is less than a given threshold value resulting from a training step. We measured the performance of the method in terms of four rates: False Acceptance Rate (FAR), False Rejection Rate (FRR), Equal Error Rate (ERR) which corresponds to the value where the FAR and FRR are equal and the Measure of Decidability (MD) which estimated the degree of separability between two distance distributions. An approximate measure of MD is given by equation (21):

$$MD = \frac{\left|\mu_1 - \mu_2\right|}{\sqrt{\frac{1}{2}(\sigma_1{}^2 + \sigma_2{}^2)}} \tag{21}$$

Where (σ_1, μ_1) corresponds to the standard deviation and mean of intra-class distribution and (σ_2, μ_2) corresponds to the standard deviation and mean of inter-class distribution

4.3 Performance evaluation of the proposed recognition system

The proposed method is based on ULGP patterns and a quality measures which take into consideration the segmentation accuracy and the quality of texture. So, we have conducted two sessions of experiments. In the first session, we apply the typical system to demonstrate the discriminating properties of the ULGP method. In the second session, we used the proposed system to prove the importance of quality score to improve the accuracy. In the following sections, we will present the performed tests and the obtained rates.

4.3.1 Evaluation of ULGP method

To evaluate ULGP method, two series of experiments are performed. In the first series of experiments, we wanted to compare the performance of parameters which can be classified in three classes:

- Parameters of Gabor filters: frequencies and orientations
- Parameters of Local Binary Patterns features: radius and neighbours number
- Parameters of features extraction: statistical feature and the choice of blocks parameters (size and overlap).

For each fixed parameters, all possible comparisons between irises are made to obtain a total number of 1706849 on Casia v3 database including 8766 of intra-class comparisons and

1698083 of inter-class comparisons. We have illustrated results by plotting DET curves (Detection Error Tradeoff) which represents the evolution of FRR against FAR for each parameter (as shown in Fig. 12). Experimental results indicate that computing ULBP with R=2 and P=16 and considering standard deviation in non-overlapping blocks of 10x10 achieve high recognition performance. The intra-class and inter-class distance distribution of optimal parameters were illustrated in Fig. 13-a. This system achieved 0.68% of EER and 3.02 % of FRR where FAR=0.
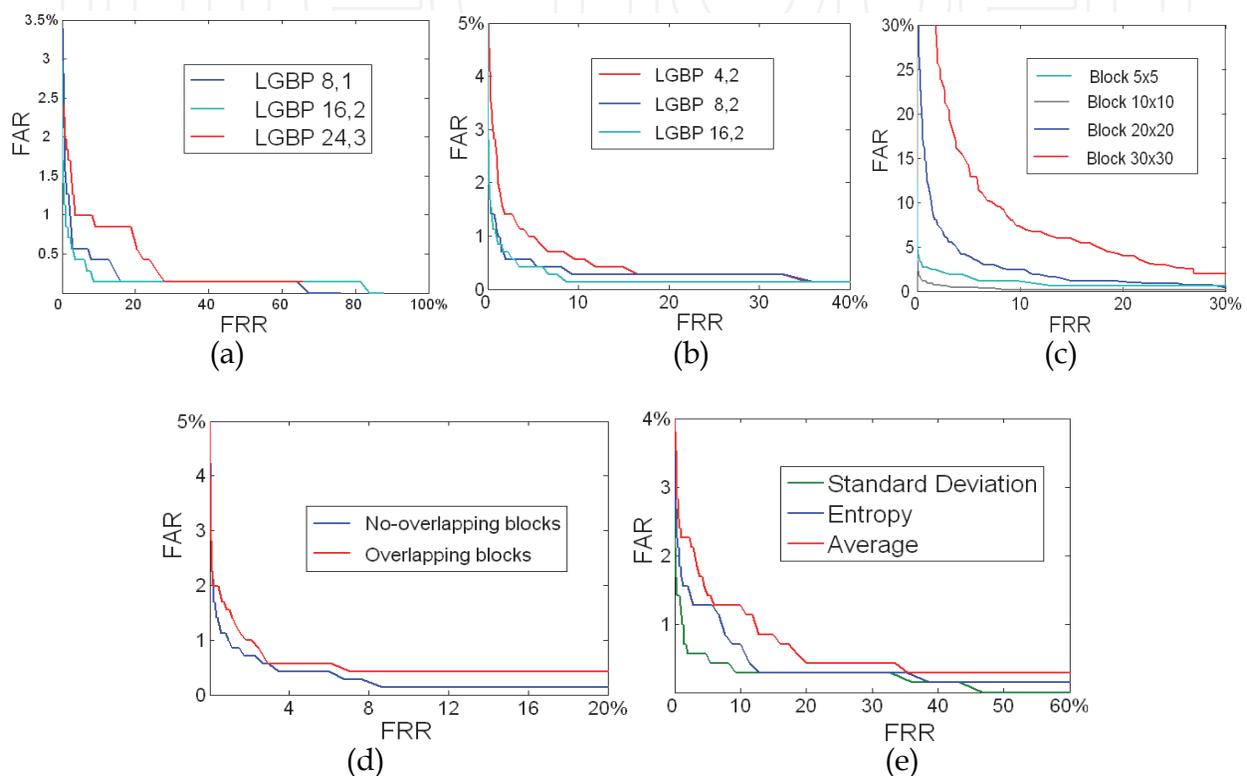
Fig. 12. DET curves for different parameters (a) ULBP rayon (b) Neighbours number (c) Block size (d) Choice of block (e) Statistical feature

In the next series of experiments, we have evaluated three other approaches:
- Application of ULBP operators on iris polar image and division of obtained image into non-overlapping blocks, then computation of statistical feature within each block.
- Generation of 16 Gabor filtered images, then for each output image, considering real part to compute statistical coefficient in extracted blocks.
- Description of iris texture by 16 Gabor filters and generation of iris signature according to "4 quadrants" coding phase.

Fig. 13 illustrate distance distribution of these experiments. As can be seen, Uniform Local Gabor Patterns ULGP perform better than others. Table 1. summarized results of evaluation of all approaches.

It has been confirmed experimentally that combining ULBP operators and Gabor filters provide a good discrimination between iris patterns and achieved higher accuracies than Gabor phase encoding.
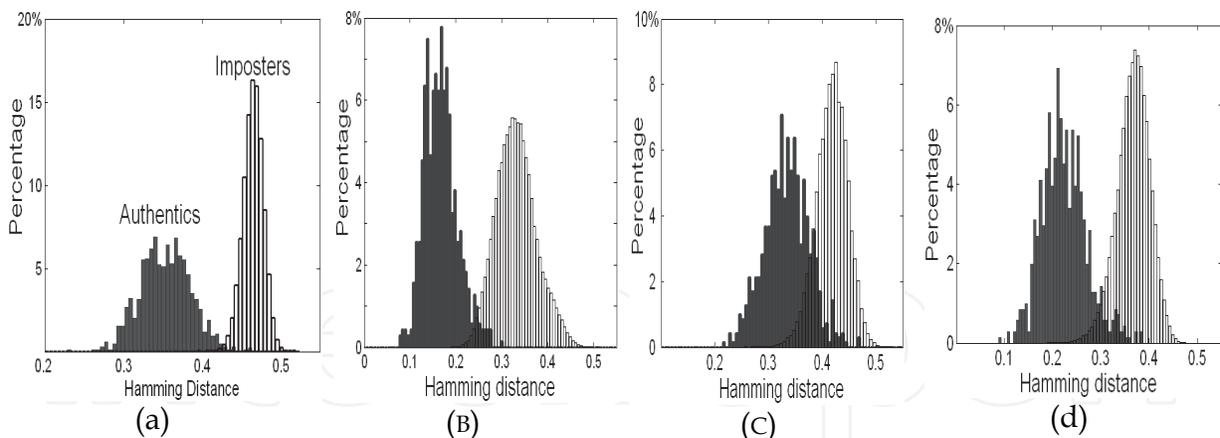
Fig. 13. Comparison between the results obtained by extraction of statistical features on
(a) ULGP representation (b) Gabor outputs (c) ULBP on iris texture (d) Coding Gabor phase

	FRR/FAR=0 (%)	EER (%)	MD
Gabor phase	31.78	4.66	3.57
Gabor	8.47	1.97	4.17
ULBP	82.7	13.93	2.08
ULGP	3.02	0.68	4.67

Table 1. Reported results from different algorithms

4.3.2 Integration of quality scores to improve performance

4.3.2.1 Validation of quality scores on iris database

We calculated quality scores Q_s, Q_t and Q for all segmented images of Casia database. The Distributions of Fig. 14 show the percentage of iris images in function of the quality level. Fig. 14-a represents the distribution of irises according to Q_s. we can see that the quality score varies between 0.32 and 1 and most images are well segmented. Also, the distribution (Fig. 14-b) shows that most images contain enough information to be identified. The score Q_t varies between 0.37 and 1.According to Fig. 14-c, we can consider that the base Casia v3 has a medium quality and Q varies between 0.39 and 1.

Based on the distribution of the quality score Q, we fixed a number of decision thresholds specifying the minimum quality to exploit the image by the system.
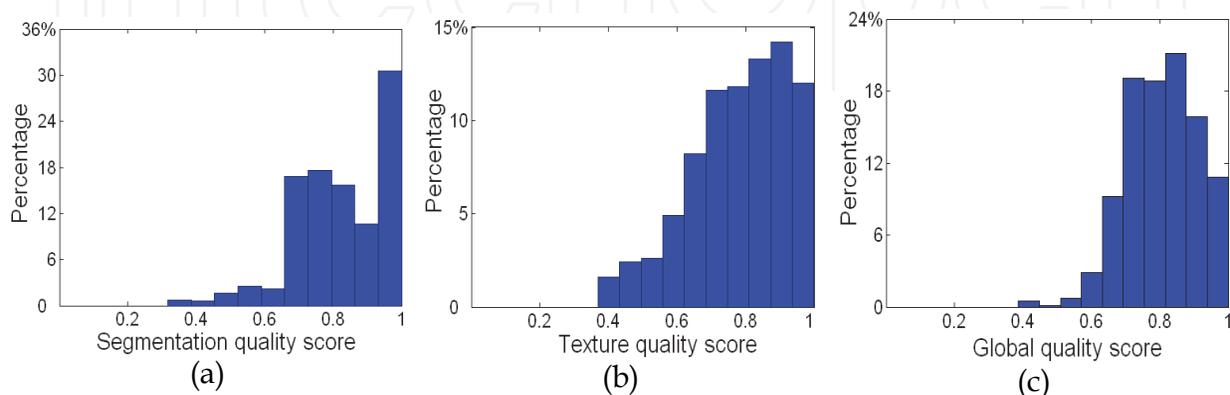

Fig. 14. Distribution of iris images based on quality index (a) Q_s (b) Q_t (c) Q

4.3.2.2 Evaluation of the proposed recognition system

After of the integration of the quality measures in the recognition system, we evaluated the system performance according to different quality thresholds. The tests are performed on iris image classes specified according to the quality thresholds defined experimentally. For each iris class, we calculated the similarity measures between all pairs of selected images. In Fig. 15, we have shown three distributions obtained by selection of images according to three quality thresholds Q: 70%, 75% and 80%.
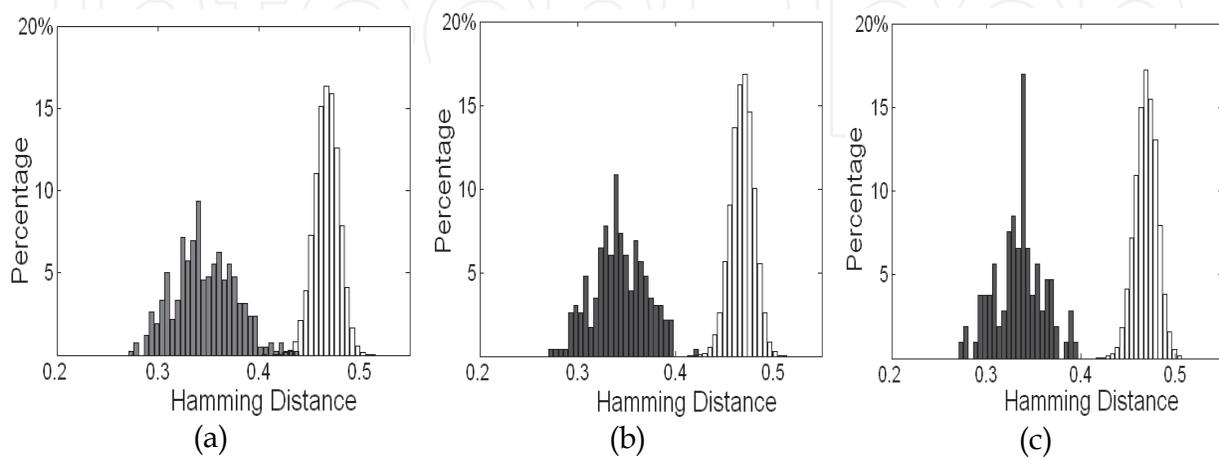
Fig. 15. Evolution of the distance distributions for different quality thresholds

By comparing these distributions with that obtained initially (Fig. 13-a) without considering the quality index, we can notice that the elimination of poor quality images improves the accuracy in the comparison. In fact, the overlap of two distributions (genuine and imposters) decreases by raising the quality level of selection. Since the threshold is set in this overlap area, we have to define a value for each class, then we verify the similarity of two irises by comparing the threshold to the distance between their feature vectors.

Based on the distributions obtained for different quality thresholds Q, we calculated the rate FAR, FRR, EER and MD for each distribution. We indicated in Table-2 the percentage of selected iris and the obtained rates for each quality threshold. We may notice an improvement of error rates by integrating the quality part in initial system and increasing the quality threshold value.

	Initial	S_1	S_2	S_3	S_4	S_5	S_6
% of database	100%	94%	85%	76%	70%	53%	36%
EER	0.68%	0.51%	0.4%	0.38%	0.16%	0.05%	0.02%
FAR/FRR=0	30.16%	28.95%	28.06%	27.22%	0.38%	0.04%	0.01%
FRR/FAR=0	3.02%	2.63%	1.48%	1.29%	0.98%	0.97%	0.85%
MD	4,67	4,83	5,01	5,04	5,17	5,34	5,52

Table 2. Reported results from proposed recognition system

5. Conclusion

In this chapter, we have presented a novel iris recognition system which combines Gabor filters and ULBP operators to characterize iris texture and a quality method to eliminate

poor quality images. First, we have used Hough transform to segment iris. Then, we have evaluated different iris borders to generate a segmentation quality score. This score is combined with a quality texture score to define a global quality measure. So, we consider in the feature extraction step only iris images which are correctly segmented and has sufficient texture information for recognition. Then, we have applied a bank of Gabor filters to extract directional texture information of the accepted iris image, then, the real part of each Gabor transformed image is converted into ULGP index map and we have computed a set of statistical measures in local regions. These features are concatenated to form the complete feature vector. Finally, we have encoded relationship between values to generate an iris template of 1920 bits. The similarity between templates is estimated by computation of the Hamming distance.

The proposed method is tested on Casia v3 iris database. Our experiments illustrate the effectiveness of ULBP to extract rich local and global information of iris texture when combined with simultaneously multi-blocks and multi-channel method. Also, obtained results show an improvement of iris recognition system by incorporating proposed quality measures in the typical system.

6. References

A.C. Bovic, M.Clarck, W.S. Geiler (1990), *Multichannel texture analysis using localised spatial filters*, IEEE Transaction, Patt. Anal. Machine Intell, Vol 12, pp 55-73, 1990.

C. Belcher, Y. Du (2008), *A selective feature information approach for iris image quality measure*, IEEE Trans. Inf. Forensics Security, Vol. 3, N°. 3, pp. 572–577, 2008.

C. L. Tissé (2003), *Contribution à la Vérification Biométrique de Personnes par Reconnaissance de l'Iris*, Phd Thesis, Montpellier II University, Octobre 2003.

CASIA Iris database (2006), *www.sinobiometrics.com*, Chinese Academy of Sciences.

E. Krichen, A. Mellakh, S. Garcia-Salicetti, K. Hamrouni, N. Ellouze, B. Dorizzi (2004). *Iris Identification Using Wavelet Packet for Images in Visible Light illumination*, 1st International Conference on Biometric Authentication, China, July 15-17, 2004.

E. Krichen (2007), *Reconnaissance des personnes par l'iris en mode dégradé*, Phd Thesis, Ecole doctorale Sitevry / Evry-Val d'Essonne University, Octobre, 2007.

H. Proença, L.A. Alexandre (2006), *A Method for the Identification of Noisy Regions in Normalized Iris Images*, IEEE 18th International Conference on Pattern Recognition ICPR, Vol. 4, pp. 405-408, Hong Kong, August 2006.

H. Qureshi, O. Sertel, N. Rajpoot, R. Wilson, M. Gurcan (2008). Adaptive Discriminant Wavelet Packet Transform and Local Binary Patterns for Meningioma Subtype Classification, International Conference on Medical Image Computing and Computer-Assisted Intervention, pp.196-204, 2008.

H. Sung, J. Lim, J. Park, Y. Lee (2004), *Iris Recognition Using Collarette Boundary Localization*, 17th Int. Conf. on Pattern Recognition, Vol. 4, pp. 857-860, 2004

J. A. Montoya-Zegarra, J. Beeck, N. Leite,R. Torres, A. Falcao (2008). *Combining global with local texture information for image retrieval applications*, 10th IEEE International Symposium on Multimedia, 2008.

J. Cambier, U. C. Von Seelen (2006), *Multi-camera Iris Quality Study*, NIST Biometric Quality Workshop, 8-9 March, 2006.

J. Daugman (1994). Biometric personal identification system based on iris analysis, US PATENT, 5291560, Mars 1994.

J. Daugman (2007), *New Methods in Iris Recognition*, IEEE Trans. Systems, Man and Cybernics – Part B: Cybernics, Vol. 37, N°.5, pp. 1167–1175, October 2007.

J. Huang, L. Ma, T. Tan, Y. Wang (2007). *Learning Based Enhancement Model of Iris*, Scientific Literature Digital Library and SearchEngine, United States, 2007.

K. Matej, J. Pers, P. Matej, S. Kovaci (2006)c, *A Bayes-Spectral-Entropy-Based Measure of Camera Focus Using a Discrete Cosine Transform*, Int. Jour. Pattern Recognition Letters, Vol. 27, N°. 13, pp. 1431-1439, October 2006.

L. Ma, Y. Wang, T. Tan (2002). *Iris recognition using circular symmetric filters*, Proceeding of 16th International Conference on Pattern Recognition, Vol 2, , pp 414-417, August 11-15, 2002.

L. Ma, T. Tan, Y. Wang, D. Zhang (2003), *Personal Identification Based on Iris Texture Analysis*, IEEE Transactions on Pattern Analysis and Machine Intelligence, Vol. 25, N°. 12, December 2003.

L. Masek (2003). *Recognition of Human Iris Patterns for Biometric Identification*, Doctorate thesis, University of Western Australia, 2003.

M. El Aroussi (2009). *Information Fusion towards a Robust Face Recognition System*, Doctorate thesis, Sciences Faculty, Rabat, Maroc, 2009.

M. Vatsa, R. Singh, A. Noore (2008), *Improving Iris Recognition Performance Using Segmentation, Quality Enhancement, Match Score Fusion, and Indexing*, IEEE Transactions on Systems, Man and Cybernetics. Part B. Cybernetics Vol. 38, N° 4, pp. 1021-1035, 2008.

N. Ahmed, T. Natarajan, K. R. Rao (1974), *Discrete Cosine Transform*, IEEE Transactions on Computers, Vol. 23, pp. 90-93, January 1974.

N. D. Kalka, V. Dorairaj, Y. N. Shah, N. A. Schmid, B. Cukic (2006), *Image Quality Assessment for Iris Biometric*, Biometric Technology for Human Identification, Vol. 6202, pp. 1..11, Florida-USA, 17-18 April 2006.

N. Feddaoui, K. Hamrouni (2009). *An efficient and reliable algorithm for iris recognition based on Gabor filters*, Transactions on Systems, Signals & Devices, Vol.5, N°.3, pp.1-17, 2010.

N. Feddaoui, K. Hamrouni (2010). *Iris recognition based on multi-block Gabor statistical features encoding,* International Conference on *Soft Computing and Pattern Recognition* SoCPaR 2010, pp. 99-104, Cergy Pontoise/Paris France, 7-10 December, 2010.

R.P. Wildes (1997), *Iris recognition: an emerging biometric technology*, Proceedings of the IEEE , Vol. 85, N°. 9, pp. 1348 -1363, September 1997.

S. Chabrier, C. Rosenberger, B. Emile (2005), *Evaluation de la performance de la segmentation d'images par fusion de critères,* 9ème congrès jeunes chercheurs en Vision par ordinateur ORASIS, Clermont Ferrand, France, 2005.

S. Lim, K. Lee, O. Byeon, T. Kim (2001). *Efficient iris recognition through improvement of feature vector and classifier*, Electronics and Telecommunications Research Institute Journal, Vol. 23, N. 2, Korea, 2001.

S. P. Foliguet, L. Guigues (2006), *Evaluation of image segmentation:state of the art, new criteria and comparison,* Journal traitement de signal, Vol. 23, N°. 2, 2006.

T. Ojala, M. Pietikainen, and D. Harwood (1996), *A comparative study of texture measures with classification based on feature distributions*, Pattern Recognition, 1996, Vol. 29, N° 1, pp. 51-59. 1996

W. B. Pennebaker, J. L. Mitchell (1992), *JPEG Still Image Data Compression Standard*, 1st Kluwer Academic Publishers Norwell, USA 1992.

W. Ketchantang, S. Derrode, L. Martin, S. Bourennane (2007), *Nouveau Descripteur Local de Qualité des Images d'Iris dans les Séquences Vidéos*, GRETSI, Troyes, 11-14 septembre 2007.

X liu (2006), *Optimizations in Iris Recognition*, A Dissertation Submitted to the Graduate School of the University of Notre Dame in Partial Fulfillment of the Requirements for the Degree of Doctor of Philosophy in Computer Science, 2006.

X. Tan, B. Triggs (2007). *Fusing Gabor and LBP Feature Sets for Kernel-Based Face Recognition*, In: Analysis and Modeling of Faces and Gestures, pp. 235–249, 2007.

Y. Chen, S. C. Dass, A.K. Jain (2006), *Localized Iris Image Quality Using 2-D Wavelets*, International Conference on Biometrics, Vol.3832, pp.373-381, Chine, January 2006

Y. Du, C. Belcher, Z. Zhou, R. Ives, *Feature correlation evaluation approach for iris feature quality measure*, International Journal of Signal Processing, Vol. 90, N°. 4, pp. 1176–1187, April 2010.

Y. Wang, Z. Mu, H. Zeng (2008). *Block-based and Multi-resolution Methods for Ear Recognition Using Wavelet Transform and Uniform Local Binary Patterns*, 19th International Conference on Pattern Recognition, Dec. 2008.

Z. Zhang, Guang, Hua, Salganicoff, Marcos (1999), *Method of Measuring the Focus of Close-up Images of Eyes*, U.S. Patent 5 953 440, 14 September, 1999.

Z. Zhou, Y. Du, C. Belcher (2009), *Transforming Traditional Iris Recognition Systems to Work in Nonideal Situations*, IEEE Trans. on Industrial Electronics, Vol.56, N°.8, 2009.

Advanced Biometric Technologies

Edited by Dr. Girija Chetty

The methods for human identity authentication based on biometrics â€" the physiological and behavioural characteristics of a person have been evolving continuously and seen significant improvement in performance and robustness over the last few years. However, most of the systems reported perform well in controlled operating scenarios, and their performance deteriorates significantly under real world operating conditions, and far from satisfactory in terms of robustness and accuracy, vulnerability to fraud and forgery, and use of acceptable and appropriate authentication protocols. To address some challenges, and the requirements of new and emerging applications, and for seamless diffusion of biometrics in society, there is a need for development of novel paradigms and protocols, and improved algorithms and authentication techniques. This book volume on â€œAdvanced Biometric Technologiesâ€ is dedicated to the work being pursued by researchers around the world in this area, and includes some of the recent findings and their applications to address the challenges and emerging requirements for biometric based identity authentication systems. The book consists of 18 Chapters and is divided into four sections namely novel approaches, advanced algorithms, emerging applications and the multimodal fusion. The book was reviewed by editors Dr. Girija Chetty and Dr. Jucheng Yang We deeply appreciate the efforts of our guest editors: Dr. Norman Poh, Dr. Loris Nanni, Dr. Jianjiang Feng, Dr. Dongsun Park and Dr. Sook Yoon, as well as a number of anonymous reviewers.

How to reference

In order to correctly reference this scholarly work, feel free to copy and paste the following:

Nadia Feddaoui, Hela Mahersia and Kamel Hamrouni (2011). Improving Iris Recognition Performance Using Quality Measures, Advanced Biometric Technologies, Dr. Girija Chetty (Ed.), ISBN: 978-953-307-487-0, InTech, Available from: http://www.intechopen.com/books/advanced-biometric-technologies/improving-iris-recognition-performance-using-quality-measures

INTECH
open science | open minds